Molecular Crystals and Liquid Crystals
Publication details, including instructions for authors and subscription information:
http://www.tandfonline.com/loi/gmcl16

Principal Electrical Conductivities in the Organic Conductors TEA.$(TCNQ)_2$ and TTF.TCNQ: The Microwave Approach

Jean Louis Miane [a] , Alain Filhol [b] , Manuel Almeida [c] & Ib Johannsen [d]

[a] Laboratoire de Physique Expérimentale, Université de Bordeaux I, 33405, Talence, France

[b] Institut Laue, Langevin, 156X, 38042, Grenoble, Cedex, France

[c] Chemistry Department, LNETI, P-2686, Sacavém Codex, Portugal

[d] Department of General and Organic Chemistry, University of Copenhagen, DK-2100, Copenhagen, Denmark

Version of record first published: 20 Apr 2011.

Mol. Cryst. Liq. Cryst., 1986, Vol. 136, pp. 317–333
0026-8941/86/1364–0317/$20.00/0

Printed in the United States of America

Principal Electrical Conductivities in the Organic Conductors TEA.$(TCNQ)_2$ and TTF.TCNQ: The Microwave Approach

JEAN LOUIS MIANE

Laboratoire de Physique Expérimentale, Université de Bordeaux I, 33405 Talence, France

ALAIN FILHOL

Institut Laue, Langevin, 156X, 38042 Grenoble-Cedex, France

MANUEL ALMEIDA

Chemistry Department, LNETI, P-2686 Sacavém Codex, Portugal

and

IB JOHANNSEN

Department of General and Organic Chemistry, University of Copenhagen, DK-2100 Copenhagen, Denmark

(*Received November 12, 1985*)

We describe a microwave technique to measure the directions and magnitude of the *principal* electrical conductivities and permittivities of organic conductors. The method is applied to single crystals of triethylammonium-bis 7,7,8,8-tetracyano-*p*-quinodimethane (TEA.$(TCNQ)_2$) and of tetrathiafulvalenium-7,7,8,8-tetracyano-*p*-quinodimethane (TTF.TCNQ). For the former, the *apriori* set of principal axes (a^*, ($a^*\wedge c$), c) is confirmed with principal conductivities of 430, 5.3 and 0.41–0.77 $\Omega^{-1}m^{-1}$ respectively. The room temperature permittivities have been measured for the first time ($\epsilon^*_a \sim 5.4$–5.5, $\epsilon^*_{a\wedge c} \sim 7.5$). For the latter it is clearly shown that the principal electrical axes are (a, b, c^*) and, in contrary to earlier d.c. data, we observe $\sigma_{c^*} < \sigma_a$ which is more consistent with the anisotropy of interchain interactions in this compound. The observed transverse and longitudinal anisotropies ($\sim 3.3\ 10^2$ and $2.8\ 10^4$ respectively) are larger than believed up to now.

Keywords: microwave, electrical conductivity, permittivity, anisotropy, organic conductors, TEA.$(TCNQ)_2$, TTF.TCNQ

I. INTRODUCTION

The large electrical conductivity anisotropy typical of organic conductors is a consequence of the intra and inter-chain coupling anisotropy. The corresponding band structure and the Fermi surface anisotropy play a major role in the physical properties of these solids. It has been demonstrated[1] that the conducting state may be stabilised to low temperatures by bi- or tri-dimensional interactions, while a quasi one-dimensional metallic state—such as in TTF.TCNQ—is often destroyed by metal-insulator instabilities at temperatures of the order of a few tens of Kelvin.

The conductivity anisotropy is thus an important but rarely known parameter. In fact compounds for which two (or even only one) transverse conductivities have been measured, are very few. Since these materials often crystallise in the triclinic symmetry, no principal axis is constraint by symmetry to a specific crystal axis and the conductivities measured along crystal growth axes by means of conventional methods (e.g. the d.c. four-probe technique) are not necessarily the principal values.*

In the following we show on TEA.$(TCNQ)_2$ and TTF.TCNQ samples that a microwave approach to principal conductivities is possible.

II. THE MICROWAVE METHOD

The method is that of Buravov and Shchegolev[3] extended to anisotropic dielectrics.[4]

II.1. Experimental set-up

The experimental set-up is made of a Gunn oscillator controlled by a Varactor (V.C.O.) which allows for a frequency scan range of $\simeq$20 MHz about the frequency corresponding to the mechanical tuning of the source ($\simeq$9400 MHz). The cavity works in transmission (TE°_{113} resonating mode), with detection via a thermistor and a microwattmeter. The transmission coefficient of the empty cavity is $T_0 = 0.25$, its resonance frequency is 9404 MHz and the quality coefficient is $Q_0 = 1000$. The quality coefficient Q_1 of the loaded

* e.g. Cooper[2] argued that the stacking axis in the Bechgaard salt $(TMTSF)_2ClO_4$ is not a principal conductivity axis.

cavity is determined from transmission measurements:

$$Q_1 = Q_0(T_1/T_0)^{1/2}$$

The sample, a single crystal glued at the end of a silicon rod able to rotate around its axis, is placed at the centre of the cylindrical resonant cavity. The presence of the rod removes the degeneracy of the resonant mode; the microwave field E_0 at the cavity center is linearly polarised in a direction perpendicular to the silicon rod.

II.2. Perturbation due to an anisotropic dielectric sample

Let us first assume that the cavity volume (V) and the microwave penetration depth are large compared with sample volume (v) and sample thickness respectively. We now define (x, y, z) a set of orthogonal axes attached to the sample, z being the rotation axis of the silicon rod holding the crystal. The microwave field axis E_0 is orthogonal to z and makes an angle β (0 to 360°) with the sample axis x.

Then the electric measurements will be made in the x, y plane in which x' and y' will be the observed orthogonal principal directions. x' and y' make an angle θ with x and y respectively (Figure 1).

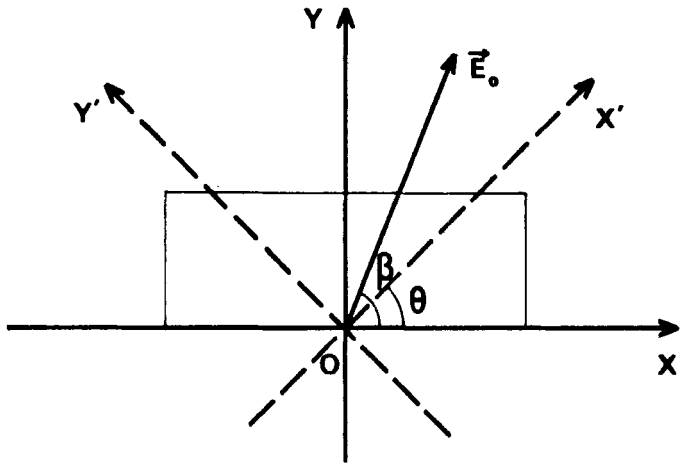

FIGURE 1 Sets of orthogonal reference axes in a plane normal to the sample rotation axis.

E_0: microwave field axis; x, y: geometric axes, the cross-section of the sample is assumed to be rectangular with x orthogonal to its long side; x', y': the principal electric axes in the x, y plane.

The sample polarisation P and the electrical field E_0^* into the sample are related through the electrical susceptibility tensor χ which is diagonal with respect to directions x' and y'. If ϵ_0 is the vacuum permittivity, the relationship is:

$$\vec{P} = \epsilon_0 \chi \vec{E}_0^* \tag{1}$$

For x, y axes (1) becomes:

$$\vec{P} = \epsilon_0 K \vec{E}_0^* \tag{2}$$

with $K = R^{-1} \chi R$, R being a rotation matrix associated with the angle θ.

The relationship between the field at centre of the perturbated ($\vec{E}_0^*$) and unperturbated ($\vec{E}_0$) cavity is also tensorial:

$$\vec{E}_0^* = \vec{E}_0 - \frac{L\vec{P}}{\epsilon_0} \tag{3}$$

with the form factor tensor

$$L = \begin{vmatrix} L_1 & 0 \\ 0 & L_2 \end{vmatrix},$$

L_1 and L_2 being the depolarisation coefficients along x and y respectively.

The empty cavity resonance is characterised by a complex frequency $\omega = \omega_0(1 + j/2Q_0)$ with ω_0 the frequency at the resonance and Q_0 a quality coefficient. The perturbation $d\omega/\omega_0$ due to a sample given by Ref. 5:

$$\frac{d\omega}{\omega_0} = -\frac{P E_0^* v}{4W} \tag{4}$$

where W is the electromagnetic energy stored in the cavity. If I is the unity tensor equations (2), (3) and (4) lead to

$$\frac{d\omega}{\omega_0} = -\frac{v}{4W} K[I - LK]^{-1} \vec{E}_0 \cdot \vec{E}_0^* \tag{5}$$

and if $A = K[I - LK]^{-1}$ we get:

$$\frac{d\omega}{\omega_0} = -\alpha[A_1\cos^2\beta + A_2\sin^2\beta + 2A_3\sin\beta\cos\beta] \tag{6}$$

with α a coefficient which, in the theory, depends on the resonance mode only ($\alpha = 2.09\ v/V$ for the TE°_{113} mode). Thus we finally get:

$$\left.\begin{aligned} A_1 &= [K_1(1 + L_2K_2) - L_2K_3^2]/D \\ A_2 &= [K_2(1 + L_1K_1) - L_1K_3^2]/D \\ A_3 &= K_3/D \end{aligned}\right\} \tag{7}$$

with $D = (1 + L_1K_1)(1 + L_2K_2) - L_1L_2K_3^2$

It is possible to reverse the relationships (7) if $A_1L_1 \neq$ and $A_2L_2 \neq 1$ to get the coefficients K_i' from the A_i's which can be measured (see equation 6):

$$\left.\begin{aligned} K_1 &= \frac{L_2(A_1A_2 - A_3^2) - A_1}{L_1L_2(A_3^2 - A_1A_2) + A_1L_1 + A_2L_2 - 1} \\ K_2 &= \frac{L_1(A_1A_2 - A_3^2) - A_2}{L_1L_2(A_3^2 - A_1A_2) + A_1L_1 + A_2L_2 - 1} \\ K_3 &= \frac{A_3(1 + L_2K_2)}{1 - A_1L_1} = \frac{A_3(1 + L_1K_1)}{1 - A_2L_2} \end{aligned}\right\} \tag{8}$$

From (8) we get the χ_i's:

$$\left.\begin{aligned} \chi_1 &= K_1\cos^2\theta + K_2\sin^2\theta + 2K_3\sin\theta\cos\theta \\ \chi_2 &= K_1\sin^2\theta + K_2\cos^2\theta - 2K_3\sin\theta\cos\theta \end{aligned}\right\} \tag{9}$$

with

$$\theta = \frac{1}{2}\mathrm{tg}^{-1}\frac{2\,Re(K_3)}{Re(K_2 - K_1)}$$

if $Re(f)$ and $Im(f)$ are the real part and imaginary part of f respectively.

In the particular case of an anisotropic medium with $\theta = 0$ then $K_1 = \chi_1$, $K_2 = \chi_2$, $K_3 = 0$ and $A_3 = 0$ and:

$$\left.\begin{aligned} \chi_1 &= K_1 = A_1/(1 - A_1L_1) \\ \chi_2 &= K_2 = A_2/(1 - A_2L_2) \end{aligned}\right\} \tag{10}$$

Since $d\omega/\omega_0 = dF/F_0 + j\, d(1/2Q)$ if we take $dF/F_0 = \delta$ and $d(1/2Q) = \Delta$ we come back to the Buravov and Shchegolev[3] expressions:

$$\left.\begin{aligned} Re(\chi_i) &= (\epsilon_i - 1) = \frac{1}{L_i} \frac{\delta_i\left(\frac{\alpha}{L_i} - \delta_i\right) - \Delta_i^2}{\left(\frac{\alpha}{L_i} - \delta_i\right)^2 + \Delta_i^2} \\ Im(\chi_i) &= \frac{\sigma_i}{\epsilon_0\omega} = \frac{\alpha}{L_i^2} \frac{\Delta_i}{(\alpha/L_i - \delta_i)^2 + \Delta_i^2} \end{aligned}\right\} \tag{11}$$

with i an index related to the $\vec{E}_0$ position ($i = 1$ if $\vec{E}_0 // \vec{x}$, i.e. $\beta = 0°$; $i = 2$ if $\vec{E}_0 // \vec{y}$ i.e. $\beta = 90°$).

In the general case, the β dependences of $1/\alpha\, dF/Fo$ and $1/\alpha\, d(1/2Q)$ are sinusoidal with extrema at:

$$\left.\begin{aligned} \beta_1 &= \frac{1}{2} tg^{-1}\left[\frac{Re(2A_3)}{Re(A_1 - A_2)}\right] \\ \beta_2 &= \frac{1}{2} tg^{-1}\left[\frac{Im(2A_3)}{Im(A_1 - A_2)}\right] \end{aligned}\right\} \tag{12}$$

If $\theta = 0$ then $\beta_1 = \beta_2 = 0$ or $\pi/2$.

The relative shift $\Delta\beta = (\beta_2 - \beta_1)$ is interpretable only in the dielectric case.

II.2. Skin effect perturbation ($\theta = 0$)

If the sample thickness is larger than the microwave penetration depth the variation (Δ) of the inverse of the quality coefficient (Q)

is a function of the sample electrical conductivity (σ) in the field direction:[6]

$$\Delta = \frac{9\pi^2 (\mu_0 \pi)^{1/2}}{2^5} \epsilon_0 F^{3/2} \frac{\delta \cdot b}{L\sigma^{1/2}} \tag{13}$$

with: b half the minor axis of an ellipsoidal sample; μ_0 the vacuum permeability; F the microwave frequency; L the depolarization coefficient; δ the frequency cavity shift which is, to a first approximation, independent from sample electrical properties. This last parameter is given by the following relationship.[7]

$$\delta = -\frac{\alpha}{L}\left[1 + \frac{L}{\alpha}\Delta\right] \quad \text{with} \quad \frac{L}{\alpha}\Delta \ll 1 \quad \text{negligible} \tag{14}$$

II.3. Application to organic conductors

The above equations are only valid either for a pure dielectric regime or a pure skin-effect regime and, in practice, the analysis is intractable for intermediate regimes. Therefore due to the large conductivity anisotropy of organic conductors care must be taken that experimental conditions are close to one of the two limit case. If the conducting chain axis is set parallel to the microwave field direction ($\vec{E}_0$), we measure $\sigma_\parallel$ which is generally large. Then equations (13) and (14) for the skin-effect regime hold. If the chain axis is set perpendicular to $\vec{E}_0$ we will measure one of the transverse conductivities ($\sigma_\perp$). If the latter is small enough we can use equation (10) corresponding to the dielectric regime.

The limit between dielectric and skin effect regime is for $\sigma \simeq 100\ \Omega^{-1}\text{m}^{-1}$. However, if $10 < \sigma < 100\ \Omega^{-1}\text{m}^{-1}$ and $\epsilon \geq 10$ simplifications occurs in the Buravov and Shchegolev expressions (11) in the case $\theta = 0$:

$$\frac{d\omega}{\omega_0} = -\frac{\alpha_i}{L_i}, \quad \epsilon \text{ is not measurable}$$

$$d\left(\frac{1}{2Q}\right) = \frac{\epsilon_0 \omega \alpha_i}{L^2 \sigma_i} \quad \text{and} \quad \sigma_i = \epsilon_0 \omega_0 \frac{(d\omega/\omega_0)_i}{L_i} \frac{1}{d\left(\frac{1}{2Q}\right)_i}$$

with i an index referring to measurement directions x and y.

One of the major problems in the microwave measurements is the evaluation of the cavity filling coefficient (α) and of the depolarisation factors (L_i). They depend on the sample shape and α is even modified by the presence in the cavity of the silicon rod holding the sample. For these reasons we have tried to obtain experimental estimates of these coefficients with the help of metallic (copper) and dielectric (germanium) standard samples.

These measurements have shown that α is a function of sample volume (v) and orientation (β) in the cavity but, as shown later, depends little on its nature (dielectric or metallic). For the orientation effect we have observed the approximate relationship:

$$\alpha(\beta) = \alpha_1 \cos^2\beta + \alpha_2 \sin^2\beta$$

and thus for each sample α_1, and α_2 can be estimated from standards cut with the same dimensions as the sample.

In a test experiment done with a germanium standard ($4.30 \times 3.40 \times 1.70$ mm^3) rotating around its long axis we have obtained:

$$\alpha_1 = 1.24\ 10^{-3} \qquad \alpha_2 = 0.91\ 10^{-3}$$

$$L_1 = 0.55 \qquad L_2 = 0.17$$

and from a copper sample:

$$\alpha_1 = 1.12\ 10^{-3} \qquad \alpha_2 = 0.97\ 10^{-3}$$

Osborn[8] charts and formula applied to an ellipsoidal volume with axis lengths equal to the above sample dimensions give:

$$L_1 = 0.55 \qquad L_2 = 0.24$$

in reasonably good agreement with the observed values. This approximation is thus satisfactory and will be used to estimate the L_i's for each real sample. The measurement of the L_i's together with the α's from the dielectric standards would have been more accurate, however, owing to sample smallness, metallic standards are easier to accurately cut at crystal dimensions by means of spark machining but, in turn, do not allow for the L_i's measurement.

III. MAGNITUDE AND DIRECTIONS OF THE PRINCIPAL ELECTRICAL CONDUCTIVITIES IN TEA.(TCNQ)$_2$

TEA.(TCNQ)$_2$ crystallises in triclinic $P\bar{1}$ symmetry (Figure 2) and thus, as already stated, no crystal direction is an obvious principal axis. However, following Ref. 9 an *apriori* set of principal axes (a^*, $c/\backslash a^*$, c) may be assumed from the crystal structure.[10] In fact this compound is very one dimensional and the TCNQ stacking axis is the highly conducting principal axis ($\sigma_{\|}$). The principal axis with lowest conductivity is expected to be normal to the (b, c) sheets of TEA cations which act as insulators between adjacent TCNQ columns in the a^* direction.

Since reliable room temperature conductivity data[9,11] are available for TEA.(TCNQ)$_2$, this compound was a good candidate to demonstrate the validity of the microwave approach to measurement of the anisotropy of electrical properties in organic conductors. This test experiment nevertheless gave a new result: the first estimate of the room temperature anisotropy of the transverse dielectric constant (ϵ) in that material.

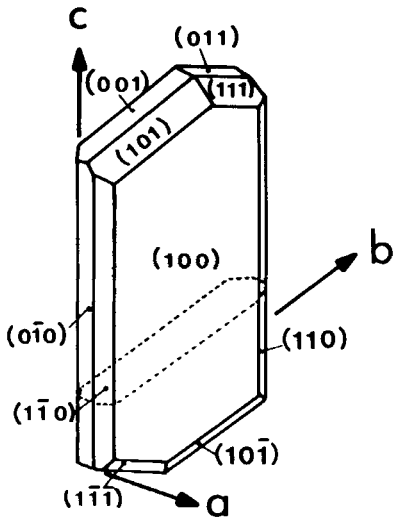

FIGURE 2 Habits of TEA.(TCNQ)$_2$ single crystals according to Refs. 22 and 12. The dashed lines indicate a {001} cleavage plane.

III.1. Experimental part

Samples were single crystals of TEA.$(TCNQ)_2$ grown from acetonitrile solution under controlled conditions[12] and showing the natural faces displayed in Figure 2. They were cleaved along {001} from crystals ≃1 mm thick along a^* to the appropriate dimensions (Table I) and glued with different orientations to the sample holder, a silicon rod.

TABLE I

Experimental results on the conductivity (σ) and the dielectric constant (ϵ) in TEA.$(TCNQ)_2$ and TTF.TCNQ

The microwave measurement of σ is, in itself, accurate but the evaluation of α_x and α_y is sensitive (up to ≃5%) to sample positioning and the estimate of L_x and L_y is rough. The ϵ determination is little accurate since it results in the difference between two quantities, one precisely known (frequency shift) and the other much less precisely (α/L).

a, b, c and a^*, b^*, c^* are the direct and reciprocal cell axis while $a' = b \wedge c^*$, $b' = c \wedge a^*$, $c' = a^* \wedge b$ with $(b, b') \simeq 20.4°$ in the case of TEA.$(TCNQ)_2$.

Sample cut axes[a] and dimensions (mm)	σ (Ω^{-1} m^{-1})	ϵ
TEA.$(TCNQ)_2$		
a^*, b', **c** 1.10; 3.00; 3.60	$\sigma_a^* = 0.77$ $\sigma_b' = 5.4$	$\epsilon_a^* = 5.40$ $\epsilon_b' = 22$[b]
a', b, $c^* = \mathbf{a} \wedge \mathbf{b}$ 0.56; 2.30; 1.20	$\sigma_a' \simeq \sigma_a^* = 0.43$ $\sigma_b = 5.7$ $\sigma_b' \simeq \sigma_b \cos(b', b) = 5.3$[c]	$\epsilon_a' \simeq \epsilon_a^* = 5.50$ ϵ_b not measurable
a*, b, c' 0.8; 3.10; 1.17	$(\sigma_b' = 10)$[d] $\sigma_c = 430$	$\epsilon_b' = 7.5$
TTF.TCNQ		
a, **b**, c^* 1.47; 7.0; 0.24	$\sigma_a = 85$ $\sigma_c^* = 1.15$	–
a, **b**, c^* 1.20; 15; 0.19	$\sigma_a = 97$ $\sigma_c^* = 1.16$	–
a, b, **c*** 1.07; 1.87; 0.05	$\sigma_a = 116$ $\sigma_b = 3.25\ 10^4$	–

[a] The sample rotation axis is bold.
[b] Error bars up to 50%–100% of the given value.
[c] This approximate relationship holds since b is nearly in the (c^*, b') plane and since σ_c is large compared with σ_b'.
[d] Biased value since b' is not parallel to a sample side.

i. Sample rotation around crystal axis c *with* $x//a^*$, $y//b' = c\wedge a^*$

In this case, the cavity filling coefficients (α_1, α_2) were measured from a copper standard cut at sample dimensions. Typical plots of δ/α and Δ/α obtained from the TEA.(TCNQ)$_2$ sample are displayed on Figure 3a. The extrema of both quantities are at $\beta = 0$ and $\beta = 90°$ and thus $\theta = 0$. As expected, this result shows, in view of equations (12), that a^* and b' are principal electric axes in the crystal plane perpendicular to the highly conducting axis c. The magnitudes of the corresponding conductivities and permittivities of the sample (Table I) were obtained using equations (11).

ii. Sample rotation around c^* *with* $x//a' = b\wedge c$ *and* $y//b$

The measurements were made with a quality coefficient of the cavity increased to $Q_0 = 4000$ by adjusting coupling holes. The experimental results show a little significant $\Delta\beta$ shift ($\simeq 5°$) and indicates that the electrical axes in the a, b plane are close to a' and b. This is again consistant to our expectations since a' is only $\simeq 1.6°$ apart from a^* while b' is $\simeq 20.4°$ from b but its projection on the b, c^* plane is only at $\simeq 0.6°$ from b.

When b is set parallel to E_0 we observe $\delta_{standard} = \delta_{sample}$ and thus, in that case, ϵ_b cannot be measured and a significant value of $\Delta\beta$ would not be interpretable via equations (12). However the dielectric equations are still valid to calculate the conductivity value from the experimental data. The obtained values of $\sigma_{a'}$, σ_b & $\epsilon_{a'}$ are given in Table I.

iii. Sample rotation around a' *with* $x//c' = a^*\wedge b$ *and* $y//b$

In contrast to previous crystal settings, the sample sides are now no longer parallel to the principal electrical directions (Table I). Thus, in agreement with the general formula (5), we observe a shift $\Delta\beta \simeq 10°$ between maxima in the $\delta/\alpha(\beta)$ curves (Figure 3b). Thus confirming that b and c' are not principal directions in the b, c plane and, in fact, we expect axes $a^*\wedge c$, c.

To check that, the value of the angle θ should be calculated from the observed value of $\Delta\beta$. However this sample orientation needs further attention since the transverse axis c is the highly conducting crystal axis. The microwave penetration depth along c (~ 0.26 mm if $\sigma_{\parallel} = 400\ \Omega^{-1}\ m^{-1}$) is smaller than the sample thickness (~ 0.8 mm) in that direction. Thus the relevant formula are those for the skin-effect regime if c is set parallel to E_0 and the dielectric formula when

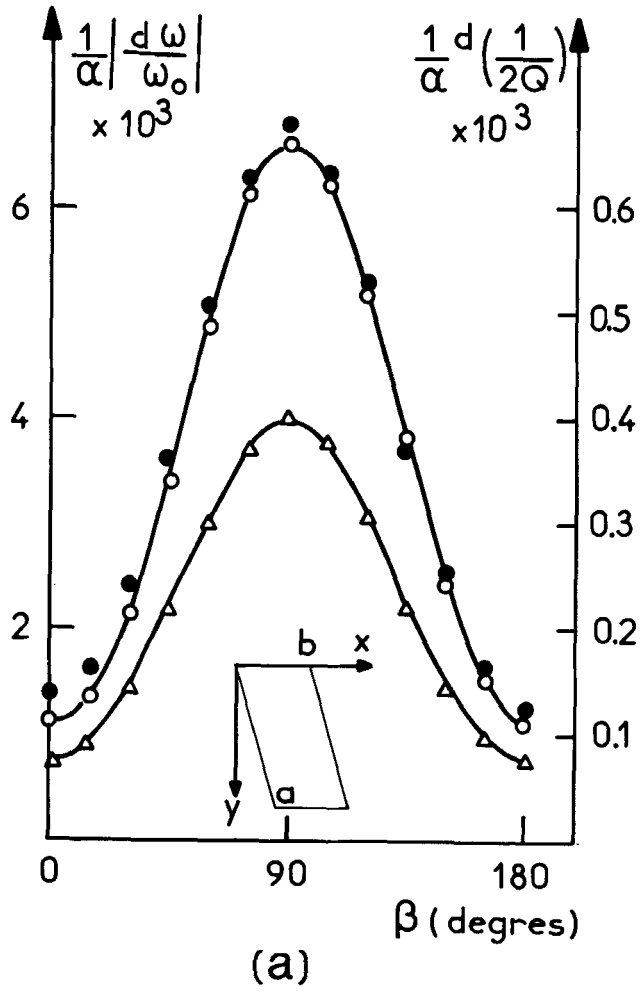

FIGURE 3 Typical plots of the observed frequency shift ($1/\alpha\ |d\omega/\omega_0|$) and of the change in the cavity quality coefficient ($1/\alpha\ d(1/2Q)$) with sample rotation.

○, ●: values of $1/\alpha\ |d\omega/\omega_0|$ observed respectively from the sample and from a copper reference with the dimensions of the latter;
△: values of $1/\alpha\ d(1/2Q)$ observed from the sample.

3a) TEA.$(TCNQ)_2$ sample rotating around c.
$\beta = 0°$ and $\beta = 90°$ if $\dot{E}_0$ is set parallel to a^* and $b' = c/\!\!\wedge a^*$ respectively.

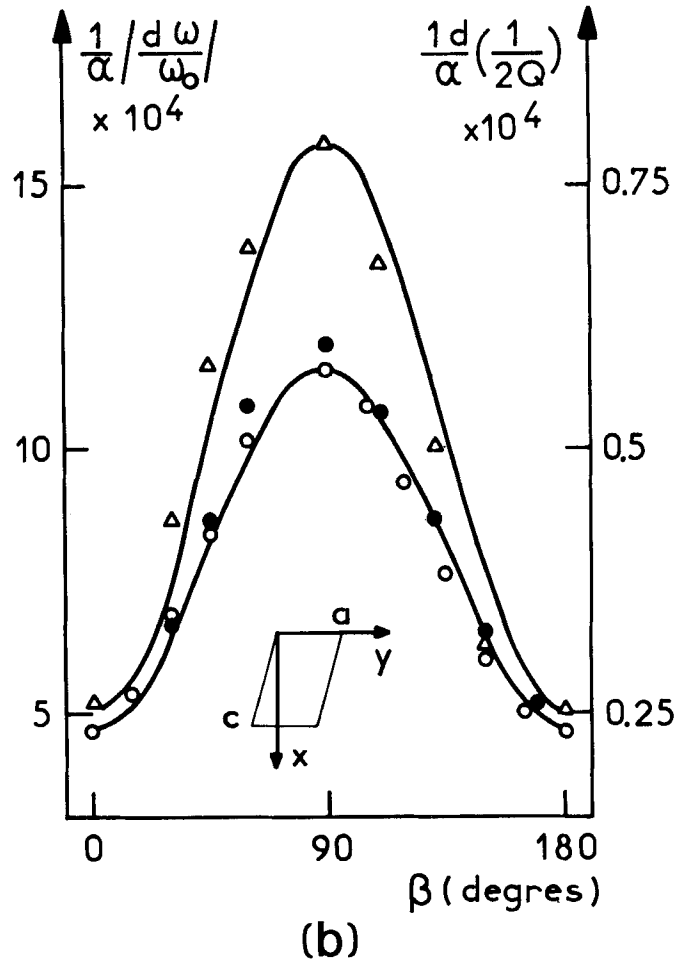

FIGURE 3 continued

3b) TTF.TCNQ sample rotating around b.
$\beta = 0$ and 90° if $\vec{E}_0$ is set parallel to c^* and a respectively.

b' is parallel to E_0. Therefore ϵ_c cannot be measured and we cannot derive θ from the above value of $\Delta\beta$ via equations (12).

The conductivities given in Table I were calculated from data with the help of equations (10, 11 and 13). However in this experiment $\theta = (b, b') = 20.4°$ while equation 11 was derived with the approximation $\theta = 0$. Indeed we observe a *bias* in the corresponding value of $\sigma_{b'}$ which is calculated larger ($10\ \Omega^{-1}\ m^{-1}$) than previous values ($5.3–5.4\ \Omega^{-1}\ m^{-1}$).

III.3. Discussion

Our values of the electrical conductivities of TEA.$(TCNQ)_2$ are in good agreement with data of the literature (Table II). However, while our value $\sigma_1 \sim 430\ \Omega^{-1}\ m^{-1}$ is in the range of the earlier data it is small compared to the $850\ \Omega^{-1}\ m^{-1}$ obtained[11] from crystals of the same origin. Since Almeida[11] also demonstrated that the room temperature conductivities (σ_1, σ_2, σ_3) of TEA.$(TCNQ)_2$ are not frequency dependent this discrepancy is probably due to sample effect.

Our values of transverse dielectric constants (ϵ_1 and ϵ_2) at room temperature are given in Table II together with low temperature data in the literature. No temperature dependence in ϵ_1 and ϵ_2 is detected but the experimental accuracy is poor.

TABLE II

Principal conductivities (σ_i) and dielectric constants (ϵ_i) in TEA.$(TCNQ)_2$

		Farges & Brau Brau & Farges[9]	Almeida[11]	This work
σ_1	$(\Omega^{-1}\ m^{-1})$	200–740[a]	850[b]	430[c]
σ_2		2.5–7	6.3	5.3–5.4
σ_3		0.8–2.6	0.11	0.41–0.77
ϵ_1	room temperature	–	–	–[c]
ϵ_2		–	–	7.5–22
ϵ_3		–	–	5.4–5.5
ϵ_1	T <120K	70 ± 20[d]	63 ± 18[e]	–
ϵ_2		–	12 ± 7	–
ϵ_3		6.2 ± 0.7	4.8 ± 0.8	–

[a] A review of earlier data.
[b] d.c. conductivity measurements.
[c] microwave 9.10^9 Hz
[d] 10^8 and 2.10^8 Hz
[e] 10^5–10^7 Hz

IV. PRINCIPAL ELECTRICAL CONDUCTIVITIES IN TTF.TCNQ

The lattice symmetry of TTF.TCNQ crystals is monoclinic $P2_1/c$.[13] As stated before, the binary symmetry axis (b), along which TTF and TCNQ ions stack, is an obvious principal axis. The two others are orthogonal and lie in the a, c crystal plane.

For this compound, *a priori* transverse principal axis are not obvious since both TTF and TCNQ columns are conductive. Further-

more the observed principal axis for a number of physical properties of TTF.TCNQ correspond to the following two sets of directions:

—(a, b, c^*): magnetic susceptibility and g factor of the EPR spectroscopy[14]

—$(b/\backslash[101], b, [101])$: EPR line width,[14] thermal expansion and isothermal compressibility.[15]

On the one hand, the first set of axes is related to molecular symmetry and a is the mean direction of strong $S \ldots N$ interchain interactions. On the other hand, theoretical predictions[16] suggest that the transverse conductivities in TTF. TCNQ have the symmetry of the phonon spectrum and thus should belong to the second set of principal axes.

IV.1. Experimental part

TTF.TCNQ samples were single crystals grown from acetronitrile.[17]

(*i*) *Sample rotation around crystal axis b with x//c*, y//a.*

Two samples were mounted accordingly. The corresponding cavity perturbations (δ_{sample}) were compared to that ($\delta_{standard}$) of metallic standards of the same shape and dimensions. To the measuring accuracy $\delta_{sample} = \delta_{standard}$ in this case and thus the sample permittivity ϵ cannot be measured but we are still in the dielectric regime for conductivity measurements.

The experimental results (Figure 3b) show that a and c^* are the principal axes since the extrema of δ/α and Δ/α are located at $\beta = 0$ and 90°. The principal conductivities are given in Table I.

(*ii*) *Sample rotation around c* with x//a, y//b*:

In this setting the anisotropy measurements are done in the a, b crystal plane where a and b are principal axes since $\beta_1 = \beta_2 = 0$. When b is parallel to E_0 the penetration depth is less than sample thickness while for a parallel to E_0 we are in the dielectric regime.

The obtained conductivities are given in Table I.

IV.2. Discussion

The microwave measurements clearly demonstrate that the principal electrical axes in TTF.TCNQ are a, b, c^* and thus the theoretical predictions from Ref. 16 are not realized. In this case, as well as in the case of TEA.$(TCNQ)_2$, the principal electrical directions are found to be related to the molecular symmetry and the conductivities depend on the intermolecular distances through the resulting transfer inte-

TABLE III

Room temperature conductivities in TTF.TCNQ

	σ_a	σ_b	σ_c^*
This work	99 ± 16	$3.25\ 10^4$	1.15–1.16
Cohen et al.[18]	50–100		400–600
Khanna et al.[19]	50	$>5\ 10^4$	–
Cooper et al.[20]	100–150	$(4 \pm 1) \cdot 10^4$	–
Thomas et al.[21] (a compilation of earlier data)	–	$2–9.2\ 10^4$	–
Anisotropy (this work)			
$\frac{\sigma_\parallel}{\sigma_a} \simeq 330$	$\frac{\sigma_\parallel}{\sigma_c^*} \simeq 28000$	$\frac{\sigma_a}{\sigma_c^*} \simeq 100$	

grals, in agreement with the ideas of Jerome.[1] The conductivities of TTF.TCNQ in the present study are given in Table III together with data in the literature. The agreement is good for σ_a and σ_b while our value of σ_{c^*} ($\sim 1.15\ \Omega^{-1}\ m^{-1}$) is much lower than the one from earlier measurement of σ_{c^*} ($400–600\ \Omega^{-1}\ m^{-1}$).[17] The latter value leads to $\sigma_a < \sigma_{c^*}$ while ours gives $\sigma_a > \sigma_{c^*}$ which is more consistent with the following facts:

—strong $S \ldots N$ interchain coupling is along a while the molecules are more separated in the c^* directions

—in similar compounds, such as HMTTF.TCNQ and HMTSF.TCNQ;* one finds $\sigma_a > \sigma_{c^*}$.

Our microwave measurements indicate a higher electrical anisotropy in the b, c^* plane ($\sigma_\parallel/\sigma_{c^*} \sim 28000$) and in the transverse plane ($\sigma_a/\sigma_c \sim 100$) of TTF.TCNQ crystals than was believed previously.

V. CONCLUSION

We have shown that the microwave technique is appropriate to the study of principal conductivities in molecular conductors. Absolute values of σ are obtained with an accuracy of about 10%, errors coming mainly from the α and L estimates.

In the present study we used samples with dimensions ($3–7\ mm^3$) which are not often available with such materials. However much

* HMTTF : Hexamethylenetetrathiofulvalene
HMTSF : Hexamethylenetetraselenafulvalene

smaller single crystals may be used and the instrument set up now allows for low temperature measurements. In fact, the thermal variation down to 20K of the conductivity and permittivity of $(TMTTF)_2SCN$ and $(tTTF)_2AsF_6$* have already been measured from samples with dimensions of about $3.0 \times 0.1 \times 0.1$ mm^3.[23] The obtained relative variations $\sigma(T)/\sigma(300K)$ of the conductivity is then obtained with an accuracy better than 5% corresponding to the experimental accuracy on dF/F and $d(1/2Q)$.

* TMTTF : Tetramethyltetraselenafulvalene
tTTF : Trimethylenetetrathiafulvalene

References

1. D. Jerome and H. J. Schulz, *Adv. Phys.*, **31**, 229–490 (1982); J. Friedel and D. Jerome, *Contemp. Physics*, **23**, 583 (1982); D. Jerome, *J. Phys.* (Paris) **44**, C3-775–780 (1983).
2. J. R. Cooper, *Mol. Cryst. Liq. Cryst.*, **119**, 121–129 (1985).
3. L. J. Buravov and I. F. Shchegolev, *Prib. Tke. Ekasp.*, **2**, 171 (1971).
4. J. L. Miane, R. Chastanet, A. Ben Salah and A. Daoud, *Phys. Stat. Sol.*, (a) **88**, 325–330 (1985).
5. J. C. Slater, *Rev. Mod. Phys.*, **18**, 441 (1946); G. Boudouris, *Ann. des Telecomm.*, **19**, 63 (1964).
6. M. Cohen, S. K. Khanna, W. J. Cunning, A. F. Garito and A. J. Heeger, *Sol. St. Commun.*, **17**, 367–372 (1975).
7. N. P. Ong, *J. Appl. Phys.*, **48**, 2935–2940 (1977).
8. J. A. Osborn, *Phys. Rev.*, **67**, 351–357 (1945).
9. J. P. Farges and A. Brau, *Phys. Stat. Sol.*, (b), **61**, 669–675 (1974); A. Brau and J. P. Farges, *Phys. Stat. Sol.*, (b), **61**, 257–265 (1974).
10. A. Filhol and M. Thomas, *Acta Cryst.*, **B40**, 44–59 (1984).
11. M. Almeida, *PhD Thesis*, Lisbon, Portugal (1982).
12. M. Almeida and L. Alcacer, *J. Crystal Growth*, **62**, 183–188 (1983); M. Almeida, L. Alcacer and A. Lindegard-Andersen, *J. Crystal Growth*, **72**, 567–577 (1985).
13. T. J. Kistenmacher, T. E. Phillips and D. O. Cowan, *Acta Cryst.*, **B30**, 763–768 (1974); A. Filhol, *Thesis*, University of Bordeaux I, France, (1985).
14. A. Maaroufi, S. Flandrois, J. Amieil and I. Johannsen, *J. Phys.*, (Paris), **44**, C3-1397–1400 (1983).
15. A. Filhol, G. Bravic, J. Gaultier, D. Chasseau and C. Vettier, *Acta Cryst.*, **B37**, 1225–1235 (1982).
16. S. Shitzkowsky, M. Weger and H. Gutfreund, *J. Phys.*, (Paris), **39**, 711 (1978).
17. Ib Johannsen, L. Groth-Andersen and K. F. Nielsen, *J. Cryst. Growth*, **51**, 627–628 (1981).
18. M. J. Cohen, L. B. Coleman, A. F. Garito and A. J. Heeger, *Phys. Rev.*, **B10**, 1298–1307 (1974).
19. S. K. Khanna, E. Ehrenfreund, A. F. Garito and A. J. Heeger, *Phys. Rev.*, **B10**, 2205–2220 (1974).
20. J. R. Cooper, D. Jerome, S. Etemad and E. M. Engler, *Sol. St. Commun.*, **22**, 257–263 (1977).
21. G. A. Thomas, et al., *Phys. Rev.*, **B13**, 5105–5110 (1976).
22. J. Jaud, D. Chasseau, J. Gaultier and C. Hauw, *C.R., Acad. Sci. Ser. C*, **278**, 769–771 (1974).
23. D. Chasseau, J. Gaultier, J. L. Miane, C. Coulon, P. Delhaes, S. Flandrois, J. M. Fabre and L. Giral, *J. Physique*, (Paris), **C3**, 1223–1227 (1983).